Brazilian Journal of Microbiology (2019) 50:859–870
https://doi.org/10.1007/s42770-019-00082-6

VETERINARY MICROBIOLOGY - RESEARCH PAPER

Disseminated melanized fungal infection due to *Cladosporium halotolerans* in a dog coinfected with canine adenovirus-1 and canine parvovirus-2

Selwyn Arlington Headley[1,2] · Mariana de Mello Zanim Michelazzo[1] · Bruno Elias[3] · Nayara Emily Viana[1] · Yuri Lima Pereira[4] · Lucienne Garcia Pretto-Giordano[5] · Jhonata Fragoso da Silva[6] · Felipe Eduardo Scardovelli da Silva[6] · Laurival Antonio Vilas-Boas[6] · Karina Keller Marques da Costa Flaiban[4] · Amauri Alcindo Alfieri[7] · Lucas Alécio Gomes[3]

Received: 13 September 2018 / Accepted: 25 February 2019 / Published online: 17 April 2019

Abstract

This report presents the pathologic findings associated with disseminated infection due to *Cladosporium halotolerans* in a dog that was simultaneously infected with canine adenovirus-1 (CAdV-1) and canine parvovirus-2 (CPV-2). A 12-year-old, mixed breed dog, with a clinical history of neurological manifestations was submitted for routine autopsy due to poor prognosis. The principal pathologic findings were mycotic necrotizing nephritis, hepatitis, and splenitis with embolic dissemination to the brain resulting in mycotic necrotizing meningoencephalitis, ventriculitis, choroid plexitis, and obstructive hydrocephalus associated with intralesional and intravascular septate pigmented fungi. PCR and sequencing of the ITS region of fungi revealed that the intralesional fungal organisms had 82% nucleotide identity with members of the *Cladosporium sphaerospermum* complex of organisms. However, a PCR assay and sequencing of the beta tubulin gene confirmed that the organism identified in this dog had 100% nucleotide sequence identity with *C. halotolerans*. Using immunohistochemistry, intralesional antigens of CAdV-1 were identified within the epithelial cells of the liver and lungs; there was positive immunolabeling for CPV-2 antigens in degenerated cardiomyocytes. These findings confirmed the active participation of *C. halotolerans* in the development of disseminated cladosporiosis in this dog and represent a rare occurrence of concomitant infection with CAdV-1 and CPV-2.

Keywords Choroid plexitis · Cladosporiosis · Dematiaceous fungi · Diagnostic pathology · Dog · Pleocytosis · Thromboembolism · Ventriculitis

Responsible Editor: Rosana Puccia.

✉ Selwyn Arlington Headley
selwyn.headley@uel.br

[1] Laboratory of Animal Pathology, Department of Veterinary Preventive Medicine, Universidade Estadual de Londrina, Rodovia Celso Garcia Cid, PR 445 Km 380, Campus Universitário, PO Box 10.011, Londrina, Paraná 86057-970, Brazil

[2] Tissue Processing Unit, Multi-User Animal Health Laboratory, Department of Veterinary Preventive Medicine, Universidade Estadual de Londrina, Londrina, Paraná, Brazil

[3] Small Animal Internal Medicine, Department of Veterinary Clinics, Universidade Estadual de Londrina, Londrina, Paraná, Brazil

[4] Laboratory of Clinical Pathology, Department of Veterinary Preventive Medicine, Universidade Estadual de Londrina, Londrina, Paraná, Brazil

[5] Laboratory of Mycology, Department of Veterinary Preventive Medicine, Universidade Estadual de Londrina, Londrina, Paraná, Brazil

[6] Laboratory of Genetics and Bacterial Taxonomy, Department of General Biology, Universidade Estadual de Londrina, Londrina, Paraná, Brazil

[7] Molecular Biology Unit, Multi-User Animal Health Laboratory, Department of Veterinary Preventive Medicine, Universidade Estadual de Londrina, Londrina, Paraná, Brazil

Introduction

Melanized fungal infections (MFI) are mycotic infectious diseases caused by darkly pigmented or dematiaceous fungi [1, 2], that produce disease in human and animals [3, 4]. The fungal disease pathogens associated with MFI include members of the genera *Capnodiales*, *Dothideales*, *Pleosporales*, *Chaetothyriales*, *Microascales*, *Sordariales*, and *Calosphaeriales* [2, 3]. These pathogens produce several clinical syndromes including cutaneous and deep localized infections, pulmonary, encephalitic, and disseminated diseases [1–3], allergic infections [2, 3], and keratitis [1] in immunocompetent and immunocompromised individuals [5]. Of these syndromes, disseminated MFI is considered as uncommon in human medicine [1, 3], with infections being predominant in immunocompromised individuals [3], but persons without any demonstratable immunodeficiency or risk factors have also been infected [2, 6]. Although an extensive review of disseminated MFI identified only 72 published cases [6], these infections have increased over the years, especially in solid organ transplants, particularly kidney transplants.

Reports of MFI described in veterinary medicine are predominant in the dog [7–12], cat, [7, 13–16] and horse [17–19], with sporadic reports in the sheep [20], and a wide range of wildlife and aquatic animals [4, 21]. An excellent review of MFI in animals can be consulted [4]. Infections due to pigmented fungi are considered as emerging opportunistic infectious diseases of animals [4], and the predisposing factors contributing to these infections in animals included ehrlichiosis [22], canine distemper virus, CDV [7], parasitic infections [21], fluid accumulation and altered flora of the infected uterus [19], environmental pollution, environmental changes [23], and stress-related conditions [4, 19, 23]. However, most reports of MFI in domestic animals [8, 9, 11–13, 15–19, 24] did not describe concomitant infections. This report describes the rare occurrence of disseminated cladosporiosis with simultaneous infections due to canine adenovirus-1 (CAdV-1) and canine parvovirus-2 (CPV-2) in a dog.

Material and methods

Location, clinical history, and autopsy

In late May 2017, a 12-year-old, female, mixed-breed dog with a clinical history of circular movement, muscular weakness of the left thoracic limb, and hyporexia was seen at the Veterinary Teaching Hospital, Universidade Estadual de Londrina (VTH-UEL), Paraná, Southern Brazil. This dog was from the outskirts of the neighboring city of Cambé and was maintained in a home with a yard space that contained a small garden. Additionally, the dog lived approximately 300 m from a grass turf producer. The dog was initially medicated with prednisolone (0.5 mg/kg, BID) and sent home; 1 week thereafter, the dog returned to the VTH-UEL with improved clinical condition and the medication was maintained. Two samples of the cerebrospinal fluid (CSF) were collected for laboratory analysis in an interval of 3 weeks: the first during the initial visit (day 1) and the other 3 weeks later (day 21). Additionally, a serum sample was collected at day 1 for the serological detection of *Toxoplasma gondii* and *Neospora caninum*. However, on the third visit 2 weeks later, the condition of the dog worsened and deteriorated rapidly thereafter; the serological assays were negative for both protozoan disease pathogens. Due to a poor prognosis, the owner elected for euthanasia and a routine autopsy was solicited to investigate the cause of the clinical disease.

Autopsy was done soon after death; tissues sections from the brain, liver, lungs, kidneys, myocardium, spleen, and small intestine were fixed by immersion in 10% buffered formalin solution and routinely processed for histopathologic evaluation with the hematoxylin and eosin stain. Selected formalin-fixed paraffin-embedded (FFPE) tissues sections of the lungs, brain, liver, myocardium, and small intestine were processed for immunohistochemical (IHC) analysis. Duplicate sections of these FFPE tissues sections were used in histochemical staining techniques to identify possible fungal and/or bacterial organisms. These histochemical techniques included the Gomori methenamine-silver (GMS) and Fontan-Masson (FM) for fungal organisms, and the Gram stain for bacteria. Additionally, sections of the cerebrum and kidney were maintained at − 80 °C until used for molecular testing.

Molecular characterization of Cladosporium spp.

Fungal DNA was extracted from frozen sections of the cerebrum and kidney by using the commercial kit Qiagen DNeasy blood & tissue kit (Qiagen Sample & Assay Technologies, Hilden, Germany) and then subjected to PCR assays that the Internal Transcribed Spacer (ITS) 1 and 2 regions by using the universal ITS 1 and 4 primers [25] and a partial fragment of the beta-tubulin gene [26]. Positive controls consisted of fungal DNA from a previous study [27]. Nuclease-free water (Invitrogen Corp., Carlsbad, CA, USA) was used as negative controls in all PCR assays.

All PCR products were separated by electrophoresis in 2% agarose gels, stained with ethidium bromide, and examined under ultraviolet light. The amplified PCR products were then purified (illustra GFX PCR DNA and Gel Band Purification Kit, GE Healthcare, Little Chalfont, Buckinghamshire, UK) and submitted for direct sequencing. The obtained sequences were examined with the PHRED software for quality analysis by chromatogram readings and were accepted if the base quality was equal to or higher than 20. Consensus sequences were

then obtained by using the CAP3 software. The obtained sequences from the PCR assays were compared by using the Basic Local Alignment Search Tool (BLAST) program (http://www.ncbi.nlm.nih.gov/BLAST) with similar sequences deposited in GenBank and with the pairwise sequence alignment software (http://www.westerdijkinstitute.nl) of the CBS fungal collection.

Immunohistochemical detection of viral pathogens of dogs

Selected FFPE tissue sections of the cerebrum, liver, lungs, and myocardium were used in immunohistochemical (IHC) assays designed to detect antigens of canine distemper virus (CDV; VMRD, WA, USA), canine adenovirus-1 (CAdV-1) and canine adenovirus -2 (VMRD, WA, USA), and canine parvovirus-2 (CPV-2; VMRD, WA, USA) as described [28]. Canine distemper was investigated since this is the principal cause of neurological disease and mortality in urban dogs from Brazil [29, 30]. Positive controls consisted of FFPE tissues from previous studies known to contain the antigens of these infectious disease pathogens [27, 28, 31]; negative controls consisted of the diluent of the primary antibodies which substituted each primary antibody in the IHC assays. Positive and negative controls were included in each IHC assay.

Results

Gross, cytological, histopathologic, and histochemical findings

The principal gross findings were observed in the kidneys, lungs, liver, spleen, and brain. Significant gross renal lesions included marked accumulation of a black-green material at the medullar region and a whitish substance at the pelvis of the left kidney (Fig. 1a); while there was a focal dark-green nodule (0.3 cm in diameter) at the cortical-medullary junction of the right kidney. There were two greenish nodules (0.8 cm in diameter) at the spleen (Fig. 1b) that extended into the sectioned surface. Several similar colored areas were observed at

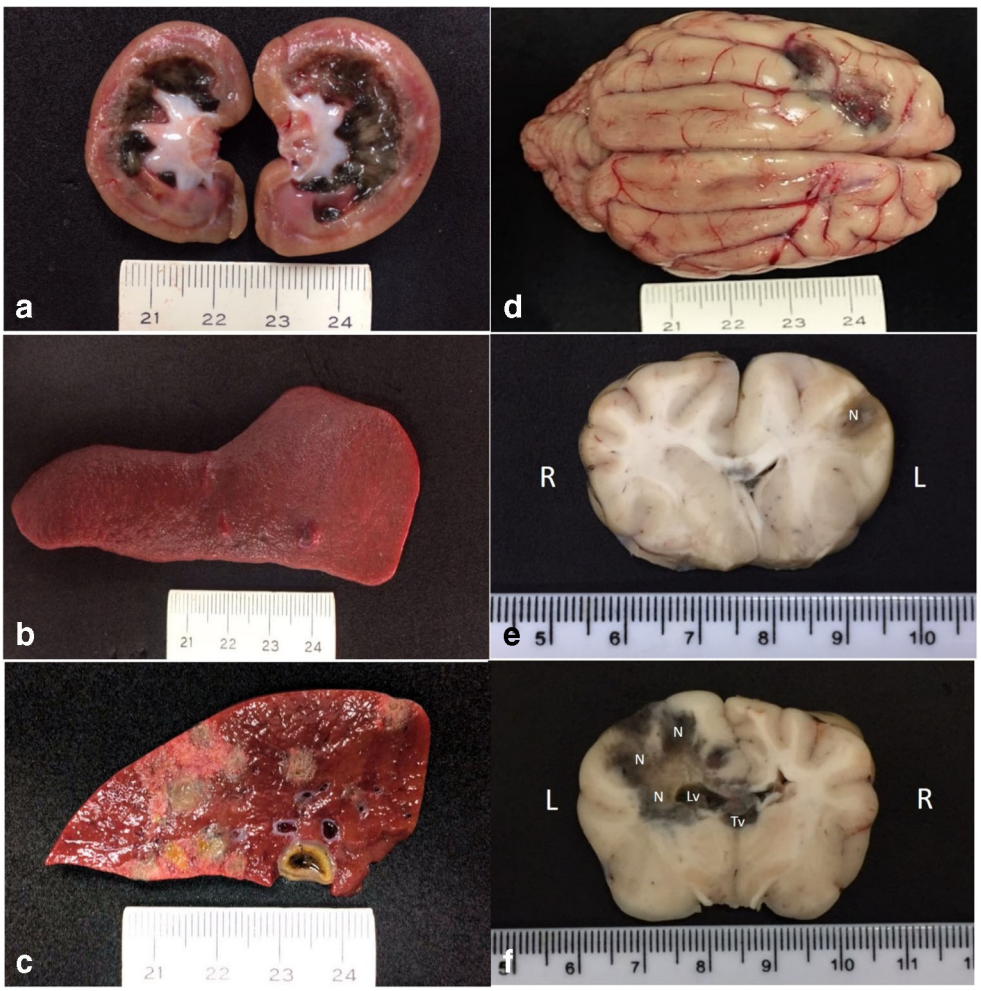

Fig. 1 Gross findings associated with disseminated phaeohyphomycosis in a mixed-breed dog. Observe the black-green accumulation within the medullary and the white substance at the pelvic regions of the left kidney (**a**) and the nodule at the spleen (**b**). There are multifocal to coalescing necrotic regions at the sectioned surface of the liver (**c**). Observe two green-black areas at the frontal lobe of the cerebrum (**d**). Transversal sections of the brain demonstrating the extension of the black-green necrotic (N) regions, which extended from the left frontal lobe (**e**) to the caudal part (**f**) of the brain (R, right; L, left). There is mild dilation of the left lateral ventricle (Lv) due to the accumulation of necrotic material; necrotic debris was also observed in the third ventricle (Tv). Scale in centimeters

the capsular and sectioned (Fig. 1c) surfaces of the liver. There was marked flattening of the gyri with narrowing of sulci and two green-black regions were observed at the left frontal lobe of the cerebrum (Fig. 1d). The sectioned surface of the cerebrum revealed severe cerebral necrosis that extended from the frontal lobe to the caudal part of brain (Fig. 1e, f). Cerebral necrosis was predominant at the left side of the cerebrum, increased in extension and severity as the cerebrum was sectioned caudally and affected both the white and gray matter. Moreover, there was mild dilation of the left lateral ventricle due to the accumulation of darkened necrotic material, which also obstructed the third ventricle. Cerebral edema was observed adjacent to the necrotic zones. The cerebellum was not affected; a transverse section through the head did not reveal any lesion at the nasal cavity.

Cytological analysis revealed branching septate hyphae from smears of the lesions of the liver and the nodules of the spleen (Fig. 2a). Histopathology revealed severe extensive renal cortical necrosis associated with intralesional accumulations of septate pigmented hyphae (Fig. 2b, c). Fungal hyphae demonstrated fine budding with diameter varying between 2.1 and 3 μm. There was massive hepatic necrosis (Fig. 2d, e) that affected most of the hepatic parenchyma associated with intralesional septate pigmented

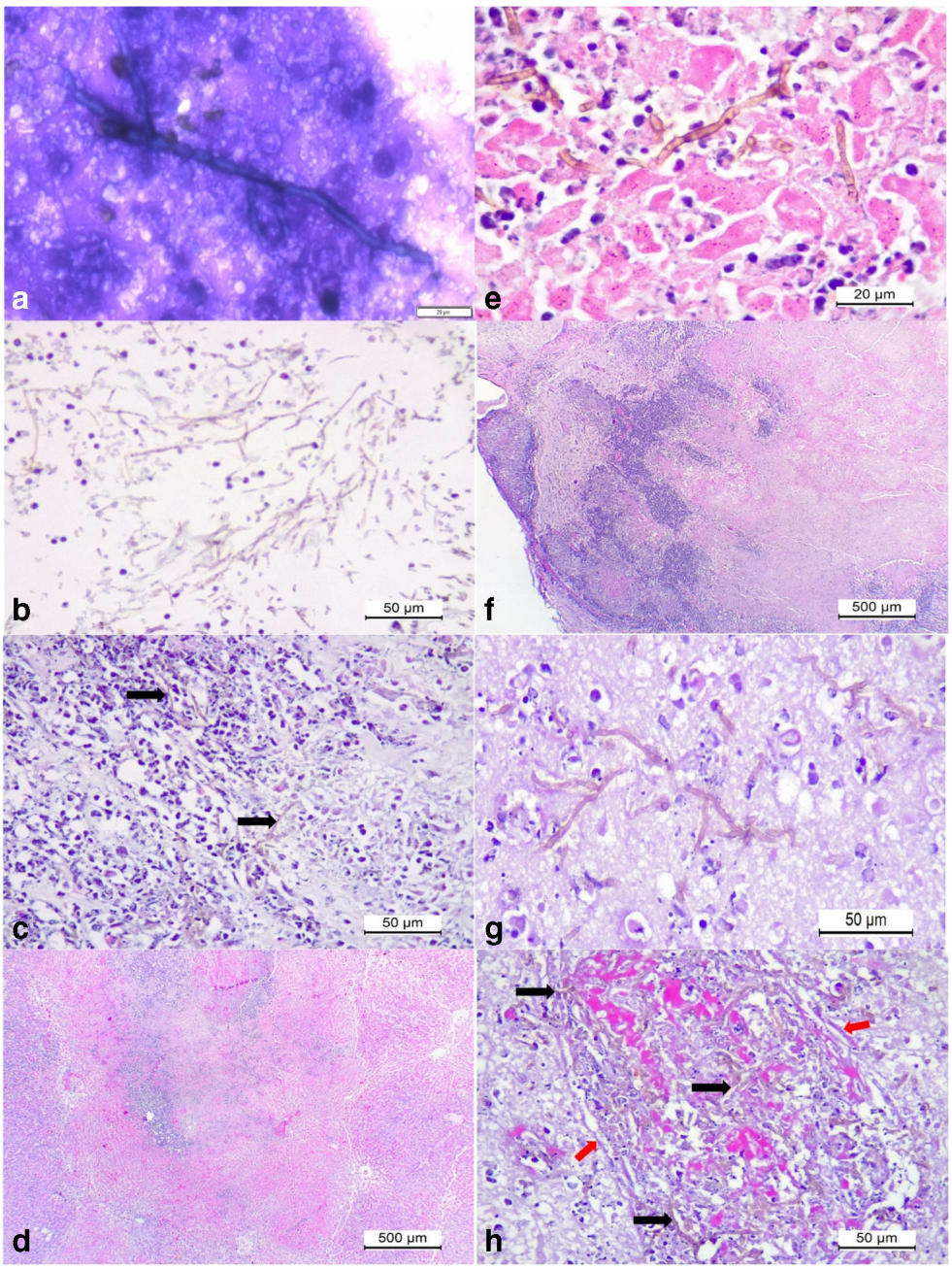

Fig. 2 Cytological and histopathologic findings associated with disseminated phaeohyphomycosis in a mixed-breed dog. Cytological smear from the splenic nodule revealed a septate fungal organism (**a**). Observe large accumulations of pigmented fungi (arrows) at the medullar region of the kidney admixed with cellular debris (**b**, **c**). There is massive hepatic necrosis (**d**) associated with intralesional-pigmented septate fungal hyphae (**e**). Observe severe cortical necrosis of the cerebrum (**f**) associated with intralesional pigmented septate fungal hyphae (**g**), and invasive vasculitis and thrombosis associated with intervascular accumulations of pigmented fungal hyphae (black arrows) within the severely destroyed wall (red arrows) of the vessel (**h**). Panoptic stain, **a**; hematoxylin and eosin stain, **b**–**h**. Bar, **a**, 20 μm; **b**, **c**, **e**, **f**, and **g**, 50 μm; **d** and **f**–**h**, 500 μm

fungi. Two principal lesions were observed at the cerebral cortex: severe extensive cortical necrosis and multifocal meningoencephalitis (Fig. 2f, g); in both lesions there were severe vasculitis and mycotic thrombosis associated with intralesional fungal hyphae (Fig. 2h); mycotic thrombosis was also observed in the kidney and liver.

Moreover, severe mycotic ventriculitis (Fig. 3a, b) was identified due to the intraventricular accumulations of myriads of pigmented septate fungal hyphae admixed with tissue debris, fibrin, and either accumulations of degenerated neutrophils or macrophages, or mixtures of both cells at the left lateral ventricle and third ventricles. Consequently, there was obstructive mycotic hydrocephalus of the lateral ventricle. The ependymocytes lining the ventricles and the choroid plexus (CP) were severely affected, being either necrotic or degenerated; in some areas, pigmented fungal hyphae transfixed the disrupted ependymal membrane of the CP and ventricles. Furthermore, there was severe mycotic necrotizing choroid plexitis and mycotic thrombosis of capillaries associated with intralesional septate pigmented fungi within the stroma of the CP at the lateral and third ventricles (Fig. 3c, e). Several capillaries within the CP were slugged with pigmented fungal hyphae, admixed with neutrophils, tissue debris, and red blood cells. In addition, there was

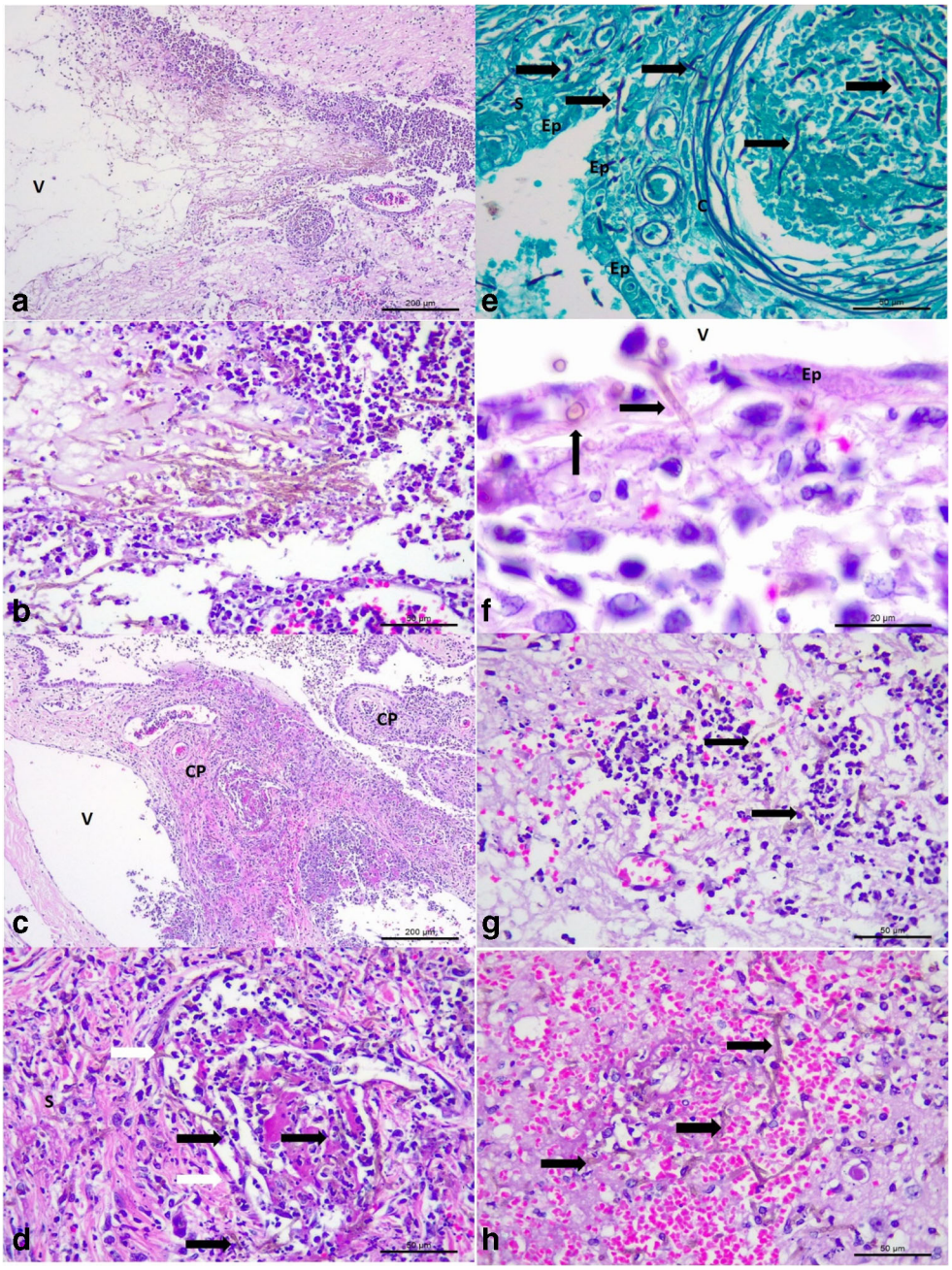

Fig. 3 Histopathologic and histochemical findings associated with mycotic ventriculitis and choroid plexitis in a mixed-breed dog. Mycotic ventriculitis: observe the dilated lateral ventricle (V) and severe accumulations of pigmented fungal septate hyphae (**a**); closer view showing the myriad of pigmented hyphae admixed with neutrophils and macrophages (**b**). Mycotic necrotizing choroid plexitis: there is severe necrosis of the stroma and ependymal cells of the choroid plexus (CP) within the lateral ventricle (V) of the brain (**a**). Closer view of the choroid plexus demonstrating a mycotic thrombosis at the stroma (S) of the choroid plexus; observe intravascular fungal hyphae (black arrows) within the stroma and a capillary (white arrows) of the choroid plexus (**d**). There is destruction of the ependymal membrane (Ep) and accumulations of fungal hyphae within a capillary (**c**) and the stroma of the choroid plexus (**e**). There are pigmented fungal organisms (black arrows) within the necrotic wall of the ependymal membrane (**f**), and within a microabscesses (**g**), and hemorrhage of the cerebrum (**h**). Hematoxylin and eosin stain, **a**–**d**, **f**–**h**; Gomori methenamine-silver histochemical stain, **e**. Bar, **a**, **c**, 200 μm; **b**, **d**, **e**, **g**, and **h**, 50 μm; **f**, 20 μm

marginalization of leukocytes across the damaged capillary wall within the CP and destruction of the ependymal layer with intraluminal accumulations of pigmented fungal organisms (Fig. 3f). At the neuropil adjacent to the ventricles, there were severe accumulations of septate brown-colored fungal hyphae, foci of mycotic vasculitis and thrombosis particularly affecting small vessels, microabscesses due to the accumulations of neutrophils with intralesional fungal hyphae (Fig. 3g), cerebral hemorrhage with intralesional septate pigmented fungal hyphae (Fig. 3h), and tissue pallor. Moreover, accumulations of septate pigmented fungal hyphae were observed at the neuropil distant from the ventricles.

All hyphae within the tissues evaluated demonstrated similar morphological characteristic as those observed in the kidney. In other regions of the liver, distant form the massive necrotic zones, there were foci of hepatocellular necrosis and paracentral areas of dilated hepatocytes suggestive of intracytoplasmic accumulations of glycogen. Other significant pathologic lesions were necrotizing bronchiolitis; rare, small nodules in the lung containing intralesional septate pigmented hyphae and foci of mild degeneration of cardiomyocytes.

The GMS histochemical stain easily identified intralesional fungal hyphae within the liver (Fig. 3a), kidney (Fig. 4b), brain (Fig. 4c), lung, and spleen of this dog; loose

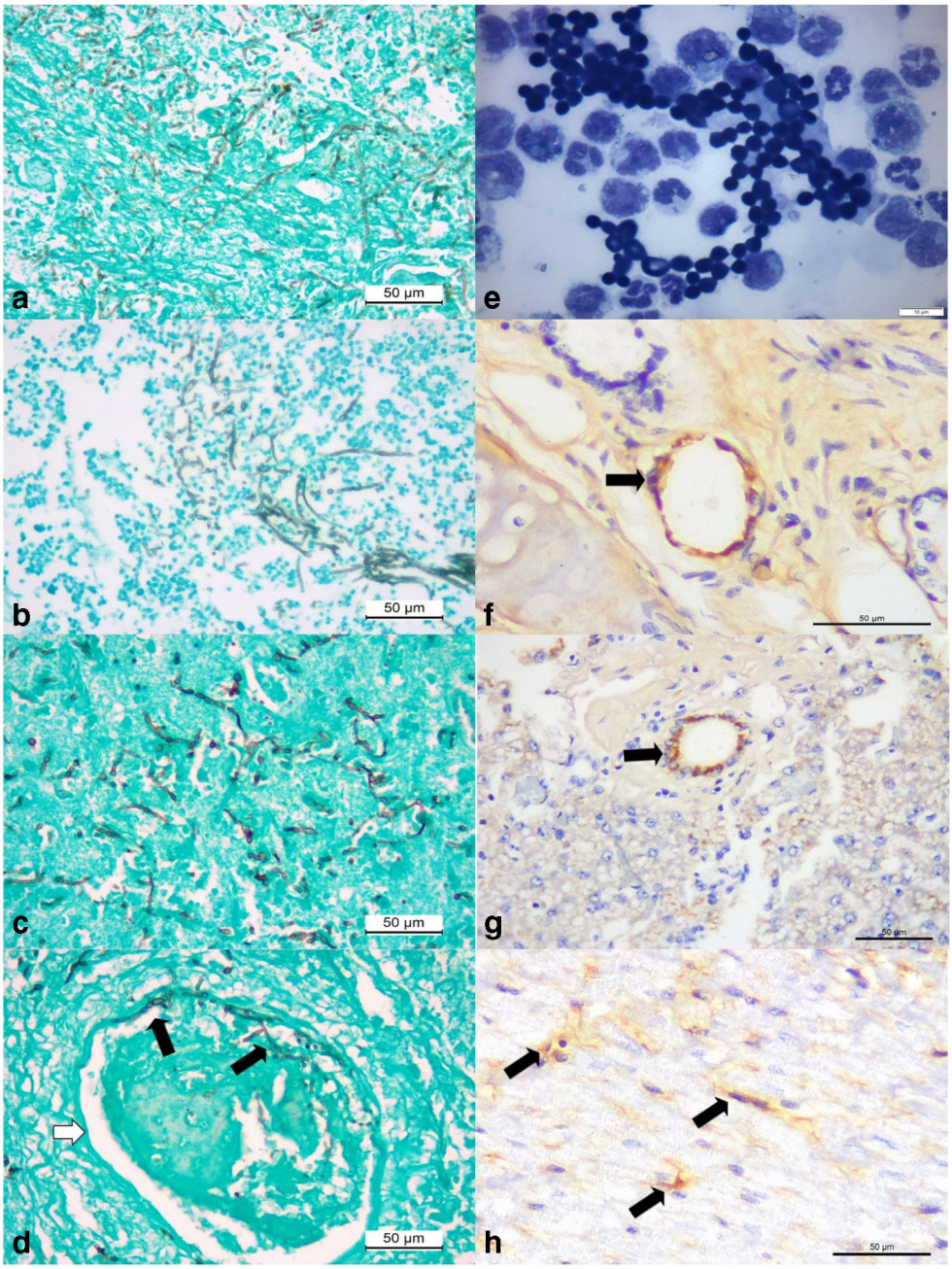

Fig. 4 Histochemical, cytological, and immunohistochemical findings of disseminated phaeohyphomycosis in a dog with simultaneous infections by canine adenovirus-1 (CAdV-1) and canine parvovirus-2 (CPV-2). Observe intralesional accumulations of septate fungal hyphae in the liver (**a**), kidney (**b**), and the cerebral cortex (**c**). There is vascular invasion of septate hyphae (black arrows) within the damaged vein (white arrow) of the cerebral cortex (**d**). Cytological evaluation of the cerebrospinal fluid revealing elevated number of fungal organisms (**e**). Immunohistochemical identification of antigens of CAdV-1 (arrows) within epithelial cells of mixed glands of the lungs (**f**) and epithelial cells of bile ducts within the liver (**g**). There is positive immunolabeling for antigens of CPV-2 (arrows) within degenerated cardiomyocytes of the myocardium (**h**). Gomori methenamine-silver histochemical stain, **a**–**d**; panoptic stain, **e**; immunoperoxidase counterstained with hematoxylin, **f**–**h**. Bar, **a**–**d**, **f**–**h**, 50 μm; **e**, 10 μm

conidiophores (3–4.7 μm in diameter) were observed forming chain-like structures and there was clear confirmation of vascular invasion by septate fungal hyphae in the cerebral cortex (Fig. 4d), kidney, and liver. Bacteria were not identified by the Gram stain in any of the tissues evaluated.

Intralesional branching septate hyphae were more readily visualized with the FM histochemical stain relative to the GMS and HE stains; with this technique, hyphae were stained brown and easily identified within sections of the brain, liver, and kidney. These septate hyphae were observed within areas of cerebral necrosis (Fig. 5a, b) and invasive fungal vasculitis (Fig. 5c), and more readily appreciated with this histochemical. Additionally, myriads of intralesional fungal hyphae were identified within the sections of the affected liver (Fig. 5d–f), and in invasive fungal hepatitis (Fig. 5f).

Clinical laboratory findings

Clinical evaluation of the CSF of the dog collected during the first visit (day 1) revealed marked increased in the protein concentration (124.9 mg/dL; physiological range, 10–27 mg/dL) with severe neutrophilic (23/mm^3; physiological range, rare) and monocytic (38/mm^3; physiological range, 0–6/mm^3) pleocytosis; bacteria and other infectious agents were not identified (Table 1). However, at day 21, there were significant increases in the protein content (5.2× threshold increase), and in neutrophilic (4.9× threshold increase) and monocytic (10× threshold increase) pleocytosis. Large accumulations of budding fungal organisms (Fig. 4e) admixed with foamy macrophages were observed in the CSF at day 21, but bacteria were not identified. These fungal structures were rounded to elliptical, varied from 2.9 to 5 μm in diameter, demonstrated fine-necked budding, and formed short chain-like structures.

Immunohistochemical detection of antigens of CAdV-1 and CPV-2

Antigens of CAdV-1 were observed within the epithelial cells of the mixed glands adjacent to pulmonary bronchi (Fig. 4f) and within epithelial cells of bile ducts of the liver (Fig. 4g) within areas of hepatocellular necrosis. Moreover, there was

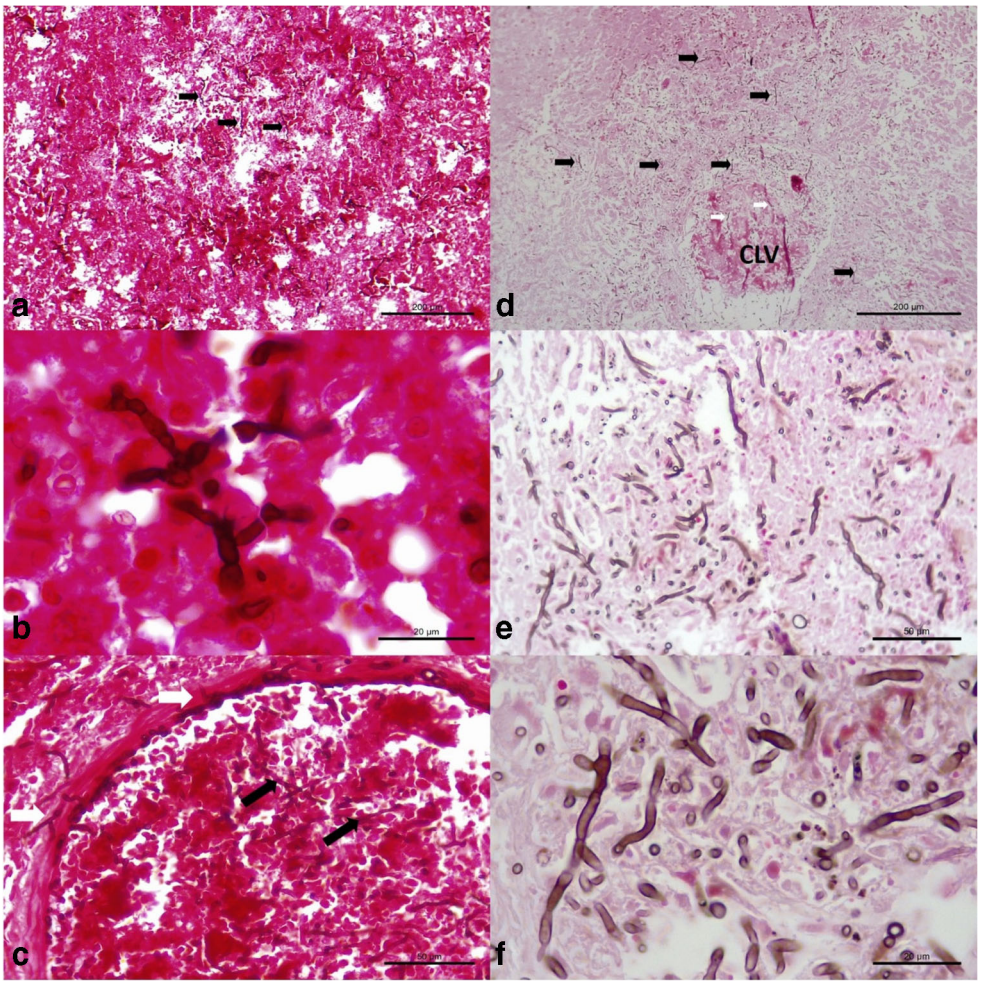

Fig. 5 Histochemical identification of intralesional septate fungal organisms in a dog with disseminated cladosporiosis. Observe intralesional pigmented fungi (black arrows) in the brain (**a**, **b**), and within an artery of the cerebrum (**c**). There are numerous accumulations of intralesional fungi in the parenchyma (black arrows) and within (white arrows) the affected central lobular vein (CLV) of the liver. Closer approximation (**e** and **f**) to demonstrate the intralesional fungal organisms within the liver. Fontana-Masson stain; bar, **a**, **d**, 200 μm; **b**, **f**, 20 μm; **c**, **e**, 50 μm

Table 1 Physical and biological characteristics of the analysis of the cerebrospinal fluid during an interval of 21 days

Physical and biological properties	Day 1	Day 21	Reference values
Color	Colorless	Colorless	Colorless
Aspect	Limpid	Slightly turbid	Limpid
Density	1006	1012	1004–1006
Glycose (mg/dL)	51	45	60–80% (serum)
Protein (mg/dL)	124.9	650.1	10–27
Red blood cells (/mm^3)	1	1	0
Nucleated cells (/mm^3)	69	507	3–6
Neutrophils (/mm^3)	23	112	Rare
Lymphocytes (/mm^3)	8	0	0–6
Monocytes (/mm^3)	38	395	0–6
Bacteria	Absent	Absent	Absent

positive immunolabeling for antigens of CPV-2 in degenerated cardiomyocytes (Fig. 4h). Antigens of CDV and CAdV-2 were not identified in any of the tissues evaluated.

Molecular identification of Cladosporium complex of organisms

The ITS primers amplified the desired partial fragments (417 base pairs, bp) of the ITS 1 and 2 regions of fungi. Blast analyses revealed that the sequences derived from this study demonstrated 82% nucleotide identity with several members of the *Cladosporium sphaerospermum* complex of organisms, including *Cladosporium* sp. strain RKSG471 (MH491831.1), *Cladosporium sphaerospermum* isolate HB (MH481610.1), *Cladosporium sphaerospermum* isolate 201805257-1 (MH424453.1), and *Cladosporium sphaerospermum* strain WL5-1A (MF422149.1). Additionally, the CBS pairwise alignment revealed that the sequence from this study had 81.1% similarity with the *Cladosporium* sp. isolates (SH216250.07; FU AY699677 and SH216250.07; FU KU579979) deposited in the CBS database.

However, the beta-tubulin PCR amplified a 388 bp fragment of the beta-tubulin gene from frozen tissue fragments of the brain and kidney of this dog. BLAST analysis revealed that the sequence derived from this study had 100% nucleotide sequence identity with examples isolates of *Cladosporium halotolerans* (EF101422.1; KT253236.1) deposited in GenBank. Furthermore, the sequences derived from this study are deposited in GenBank (ITS, Accession # MH667606; Beta-tubulin, MK533454).

Discussion

The histopathologic findings of pigmented septate hyphae in several organs of this dog support a diagnosis of disseminated MFI, since confirmation of MFI is based on the histological identification of pigmented/dematiaceous intralesional hyphae [4, 32]. Moreover, most of the lesions observed in this dog were previously identified in other domestic animals with MFI [10, 11, 14, 15, 19]. Confirmation that the dematiaceous mold involved in this case is part of the *Cladosporium* complex of organisms was achieved due to PCR assay with direct sequencing resulting in elevated nucleotide identity with known members of the *C. sphaerospermum* species complex; this methodology is recommended to effectively characterize the type of pigmented fungi associated with the development of MFI [1, 4, 6]. However, despite this similarity, we were unable to determine the exact species of *Cladosporium* associated with the disseminated disease in this dog. Nevertheless, the best match during the BLAST and CBS analyses suggested that the intralesional fungal hyphae associated with the disseminated disease are part of the *C. sphaerospermum* complex of organisms. However, the beta-tubulin PCR indicated that the isolate derived from this study had 100% nucleotide sequence identity with *C. halotolerans*. Consequently, the molecular investigation confirmed that this dog was infected by *C. halotolerans*. The molecular identification of *Cladosporium* organisms can be difficult considering that new members of this genus are continually identified in association with infectious disease of humans and animals [33]. A study done in the USA revealed that 40% (37/92) of filed isolates were identified only at the genus level by a combination of several target genes [34]; these authors suggested that the unidentified isolates could have been unclassified/new linages of *Cladosporium*, considering that there are 169 species that are considered as true members of the *Cladosporium* complex of organisms [35]. In this case, a complete molecular characterization was only achieved after the utilization of a PCR assay that targeted a specific gene. Consequently, several genes must be targeted to effectively identify the species of

Cladosporium involved in the development of disease in domestic animals.

The mixed pleocytosis (neutrophilic and monocytic) observed during the evaluation of the CSF of this animal is frequently identified in dogs with neurological manifestations of cryptococcosis [36], and sporadically in other disease such as canine blastomycosis [37]. Nevertheless, pleocytosis due to mycotic infections in domestic animals may not be frequently diagnosed. A similar scenario seems to occur in human medicine, since a retrospective study that evaluated 1,058 CSF samples only identified fungal pleocytosis in seven of these [38]. Additionally, fungal organisms were only identified during the second evaluation of the CSF; mycotic invasion of the CSF in dogs were described in infections due to *Xylohypha bantiana* [22] and *Blastomyces dermatitidis* [37]. However, it seems as if though most fungal organisms other than members of the *Cryptococcus* complex are not commonly observed during the CSF analysis of domestic animals [36, 39]. We believe that in this case, the absence of fungal organisms during the first evaluation of the CSF was probably because the infection with associated cerebral necrosis was initially localized at the frontal lobe; in humans, cerebral cladosporiosis predominantly affects the frontal lobe [40–42]. We theorize that infection spread rapidly to the caudal portions of the cerebrum resulting in mycotic meningoencephalitis with vasculitis and thrombosis, mycotic obstructive ventriculitis and hydrocephalus, considering the anatomical features of the ventricular system [43]; mycotic thrombosis as occurred in this dog is a prominent feature of *Cladosporium*-associated brain disease in humans [41]. Impairment to the ventricular system then facilitated the accumulation and consequent identification of fungal organisms within the CSF 21 days after the onset of cerebral disease. Alternatively, it was proposed that in cryptococcal encephalitis fungal proliferation occurs predominantly in the neuropil and not the CSF, and the elevated accumulations of cryptococcal organisms in the CSF may be associated with the spill over effect from cryptococcal meningitis and encephalitis [43]; consequently, this mechanism may explain the elevated concentration of fungal organisms in the CSF of this dog, due to the anatomical connections of the ventricular system of the brain [43]. Supporting evidence for the delay in fugal identification in the CSF can be associated with the significant increase in the threshold of pleocytosis and protein concentration during the 21 day period; since elevation in CSF protein concentration is associated with severe inflammation and destruction of the neuropil [39], as observed in this dog. Moreover, obstructive hydrocephalus is frequently fatal and results in rapid deterioration of the clinical status of the affected animal [36], as occurred in the case herein described, and is a frequent manifestation of human encephalitic cladosporiosis [41].

Although we have not identified other cases of mycotic ventriculitis associated with the *Cladosporium* complex of organisms in domestic animals, human cerebral cladosporiosis is a rare disease with predilection for the frontal lobe resulting in meningitis, ventriculitis, and obstructive hydrocephalus [41]. Nevertheless, mycotic ventriculitis in domestic animals was associated with infections due to *B. dermatitidis* in the dog [36, 37, 44] and *Cryptococcus neoformans v. grubii* in ruminants, [45, 46] which were confirmed by diagnostic imaging [37] and routine autopsy with histopathologic evaluations [44–46]. Blastomycosis ventriculitis in dogs is considered as the manifestation of a systemic disease [36], with associated lesions occurring in the lungs, pituitary gland, and lymph nodes [44]. Additionally, in both cases of cryptococcal ventriculitis, there were disseminated involvement at several anatomical regions of the brain [45, 46], with associated pulmonary disease in one of these ruminants [46]. In the case herein described, cladosporiosis was systemic. Although there are few cases of mycotic ventriculitis in domestic animals, initial evidence suggests that this lesion may be part of a systemic disease.

Another interesting finding during this study was mycotic choroid plexitis with vasculitis and thrombosis associated with disseminated infection due to intralesional *C. halotolerans*. Although similar descriptions of mycotic choroid plexitis were not located in the veterinary literature, vasculitis was described in previous cases of MFI in domestic animals [9, 11, 20, 47]. The choroid plexuses are formed by epithelial cells, are located within the four ventricles of the brain, and have as their primary function the production of CSF [48]; therefore, accumulations of fungal organisms within the CSF is dependent on the integrity of the ependymal cells of the CP. Even though fungal choroid plexitis was associated with infection due to *Cryptococcus* organisms in humans [49, 50], the participation of the blood-CSF barrier (BCSFB), formed by the epithelial cells of the CP, in the dissemination of fungal organisms to the brain was considered insignificant [48]. Alternatively, destruction to the blood-brain barrier (BBB) is more frequently associated with invasion of fungal organisms to the brain [48]. However, during this study, there was multifocal mycotic thrombosis and vasculitis of capillaries within the CP and destruction of the ependymal layer due to intralesional fungal hyphae, so the participation of the BCSFB in the dissemination of fungal organisms in this case cannot be totally disregarded; vasculitis and thrombosis were also described in human cryptococcal choroid plexitis [49].

The exact route of infection in this dog remains obscure, since pulmonary involvement was minimal, and lesions were not observed at the nasal cavity. This suggests that infection did not occur via inhalation, which is one of the main forms of contamination by pigmented molds [3]. Inhalation would have been the more likely form of entry in this case, considering that the dog inhabited a yard space, lived within the proximity of a grass turf dealer, and that *Cladosporium* members are environmental contaminants [35]. Additionally,

C. halotolerans was previously identified from several human body tissues, the skin of a marine mammal [34], as well from a saline solution [33], and was one of the most frequent fungal organisms identified within damp buildings [51]. Nevertheless, we believe that the lesions observed in this dog were primarily renal and hepatic, with subsequent encephalitic dissemination after destruction of the BBB [48], and possibly to a lesser extent the BCSFB. Lesions to both blood barriers were easily identified due to mycotic thrombosis and vasculitis of the neuropil and the CP, confirming an invasive fungal infection [52]. Non-pulmonary involvement, as herein described, was reported in other cases of MFI in domestic animals [7–11, 53]. Additionally, several reports of MFI in domestic animals [8–10], have suggested hematogenous dissemination to the brain after renal colonization as the probable form of encephalitic involvement, and may have occurred in the case under discussion. Subcutaneous invasion due to trauma is another principal via of infection in MFI [3], but no history of trauma was reported by the owner of this dog and traumatic lesions were not observed during autopsy. However, cutaneous invasion seem to be the primary form of contamination in cases of human cerebral cladosporiosis [41] and MFI of animals [23].

During this investigation, there were concomitant infections with CAdV-1 and CPV-2 due to consistent pathologic alterations associated with the intralesional identification of antigens of these disease agents in tissues of this dog, thereby resulting in triple infections. We have frequently diagnosed concomitant infections in puppies [27, 28, 31]; in one study, a puppy was infected by five infectious disease pathogens [31], while in another investigation four puppies were simultaneously infected by four pathogens [28]. Concomitant infections in puppies occur probably due to the immature immunological system of these animals, so the advanced age of this dog might have contributed towards the occurrence of the simultaneous infections in this case. Although the viral pathogens identified in this adult dog are not recognized as classical immunosuppressive agents, CPV-2 produces lymphopenia and subsequent immunosuppression in dogs [54], and may have contributed to the development of MFI in this animal and should be considered as a possible risk factor for the occurrence of MFI; additional risk factors were identified in animals with MFI [7, 19, 21, 22]. It must be highlighted that CDV is a well-known immunosuppressive agent of dogs, but lesions or antigens of CDV were not identified in any tissue evaluated. Alternatively, risk factors [42] or pre-existing debilitating conditions [40] were not identified in most human patients with cerebral cladosporiosis; encephalitic MFI occurs predominantly in immunocompetent individuals [3, 5]. Additionally, a review of published cases of human cerebral MFI revealed that 51.5% (52/101) of these had no associated risk factor [5]. Therefore, the advanced age of the dog coupled with the immunosuppressive effects of CPV-2 [54] may have contributed towards the development of the triple infections observed in this animal. Moreover, the melanin that is contained in the wall of all pigmented fungi can act as virulence factor in the development of MFI particularly in immunocompetent individuals [2, 3, 5], by evading the immune system of the affected host [5], and may be another key issue to explain the surgence of the multiple diseases in this dog.

Additionally, intralesional pigmented fungal hyphae were more easily identified with the FM staining technique when compared with the GMS histochemical stain and the routine HE technique. The FM stain is recommended for the identification of pigmented fungal organisms, since this technique identifies melanin that is contained within the wall of dematiaceous fungi and imparts a characteristic black to brown color to the intralesional fungal hyphae [2, 32, 55]. In this case, fungal hyphae were visualized by the HE and GMS methods and in association with the related molecular results would have been adequate to obtain a diagnosis of disseminated dematiaceous infection [32]. However, in the absence of molecular confirmation, the FM stain must be used to efficiently identify pigmented fungi, since melanin is also within the wall of additional fungal organisms such as *Aspergillus* spp. [2], *Mucorales* spp., and *Trichosporon* spp. [2, 32], and consequently can result in inaccurate histopathologic interpretations.

In conclusion, this paper describes the pathologic findings associated with disseminated cladosporiosis in a dog coinfected with CAdV-1 and CPV-2. The via of contamination and consequent development of canine cladosporiosis remains obscure, but the pathologic findings suggest hepatic and renal colonization with subsequent haematogenous encephalitic dissemination via mycotic thromboembolism.

Acknowledgements Selwyn A. Headley and Amauri A. Alfieri are recipients of the National Council for Scientific and Technological Development (CNPq; Brazil) fellowships and grants. The authors thank the owner of this dog for permission to use this animal during this report and Dr. Kerlei Cristina Medici for the realization of the beta-tubulin PCR assay.

Compliance with ethical standards

Ethical approval All applicable international, national, and/or institutional guidelines for the care and use of animals were followed.

References

1. Brandt ME, Warnock DW (2003) Epidemiology, clinical manifestations, and therapy of infections caused by dematiaceous fungi. J Chemother 15(sup2):36–47
2. Wong EH, Revankar SG (2016) Dematiaceous molds. Infect Dis Clin N Am 30(1):165–178
3. Revankar SG, Sutton DA (2010) Melanized fungi in human disease. Clin Microbiol Rev 23(4):884–928

4. Seyedmousavi S, Guillot J, de Hoog GS (2013) Phaeohyphomycoses, emerging opportunistic diseases in animals. Clin Microbiol Rev 26(1):19–35
5. Revankar SG, Sutton DA, Rinaldi MG (2004) Primary central nervous system phaeohyphomycosis: a review of 101 cases. Clin Infect Dis 38(2):206–216
6. Revankar SG, Patterson JE, Sutton DA, Pullen R, Rinaldi MG (2002) Disseminated phaeohyphomycosis: review of an emerging mycosis. Clin Infect Dis 34(4):467–476
7. Dillehay DL, Ribas JL, Newton JC Jr, Kwapien RP (1987) Cerebral phaeohyphomycosis in two dogs and a cat. Vet Pathol 24(2):192–194
8. Poutahidis T, Angelopoulou K, Karamanavi E, Polizopoulou ZS, Doulberis M, Latsari M, Kaldrymidou E (2009) Mycotic encephalitis and nephritis in a dog due to infection with *Cladosporium cladosporioides*. J Comp Pathol 140(1):59–63
9. Giri DK, Sims WP, Sura R, Cooper JJ, Gavrilov BK, Mansell J (2011) Cerebral and renal phaeohyphomycosis in a dog infected with *Bipolaris* species. Vet Pathol 48(3):754–757
10. Uchôa ICP, Santos JRS, APd S et al (2012) Feo-hifomicose sistêmica em cão. Cienc Rural 42:670–674
11. Rothenburg LS, Snider TA, Wilson A, Confer AW, Ramachandran A, Mani R, Rizzi T, Nafe L (2017) Disseminated phaeohyphomycosis in a dog. Med Mycol Case Rep 15:28–32
12. Spano M, Zuliani D, Peano A, Bertazzolo W (2018) *Cladosporium cladosporioides*-complex infection in a mixed-breed dog. Vet Clin Pathol 47(1):150–153
13. Bouljihad M, Lindeman CJ, Hayden DW (2002) Pyogranulomatous meningoencephalitis associated with dematiaceous fungal (*Cladophialophora bantiana*) infection in a domestic cat. J Vet Diagn Investig 14(1):70–72
14. Elies L, Balandraud V, Boulouha L, Crespeau F, Guillot J (2003) Fatal systemic phaeohyphomycosis in a cat due to *Cladophialophora bantiana*. J Vet Med A Physiol Pathol Clin Med 50(1):50–53
15. Simmons JK, McManamon R, Rech RR, Phillips AE, Howerth EW (2010) Pathology in practice. Necrotizing pyogranulomatous meningoencephalitis with intralesional fungal hyphae, consistent with *Cladophialophora bantiana*. J Am Vet Med Assoc 236(3):295–297
16. Evans N, Gunew M, Marshall R, Martin P, Barrs V (2011) Focal pulmonary granuloma caused by *Cladophialophora bantiana* in a domestic short haired cat. Med Mycol 49(2):194–197
17. Coles BM, Stevens DR, Hunter RL (1978) Equine nodular dermatitis associated with *Alternaria tenuis* infection. Vet Pathol 15(6):779–780
18. Genovese LM, Whitbread TJ, Campbell CK (2001) Cutaneous nodular phaeohyphomycosis in five horses associated with *Alternaria alternata* infection. Vet Rec 148(2):55–56
19. Rantala M, Attia S, Koukila-Kahkola P et al (2015) *Cladophialophora bantiana* as an emerging pathogen in animals: case report of equine endometritis and review of the literature. J Clin Microbiol 53(9):3047–3053
20. Haligur M, Ozmen O, Dorrestein GM (2010) Fatal systemic cladosporiosis in a merino sheep flock. Mycopathologia. 170(6):411–415
21. Domiciano IG, Domit C, Trigo CC, de Alcântara BK, Headley SA, Bracarense APFRL (2014) Phaeohyphomycoses in a free-ranging loggerhead turtle (*Caretta caretta*) from Southern Brazil. Mycopathologia. 178(1–2):123–128
22. Schroeder H, Jardine JE, Davis V (1994) Systemic phaeohyphomycosis caused by *Xylohypha bantiana* in a dog. J S Afr Vet Assoc 65(4):175–178
23. Seyedmousavi S, Bosco SMG, de Hoog S, Ebel F, Elad D, Gomes RR, Jacobsen ID, Jensen HE, Martel A, Mignon B, Pasmans F, Piecková E, Rodrigues AM, Singh K, Vicente VA, Wibbelt G, Wiederhold NP, Guillot J (2018) Fungal infections in animals: a patchwork of different situations. Med Mycol 56(suppl_1):165–187
24. Coldrick O, Brannon CL, Kydd DM, Pierce-Roberts G, Borman AM, Torrance AG (2007) Fungal pyelonephritis due to *Cladophialophora bantiana* in a cat. Vet Rec. 161(21):724–727
25. White T, Bruns T, Lee S, Taylor J (1990) Amplification and direct sequencing of fungal ribosomal RNA genes for phylogenetics. In: Innis M, Gelfand D, Sninsky J, White T (eds) PCR protocols: a guide to methods and applications. Academic, San Diego, pp 315–322
26. Glass NL, Donaldson GC (1995) Development of primer sets designed for use with the PCR to amplify conserved genes from filamentous ascomycetes. Appl Environ Microbiol 61(4):1323–1330
27. Headley SA, Pretto-Giordano LG, Lima SC, Suhett WG, Pereira AHT, Freitas LA, Suphoronski SA, Oliveira TES, Alfieri AF, Pereira EC, Vilas-Boas LA, Alfieri AA (2017) Pneumonia due to *Talaromyces marneffei* in a dog from southern Brazil with concomitant canine distemper virus infection. J Comp Pathol 157(1):61–66
28. Headley SA, Oliveira TES, Pereira AHT, Moreira JR, Michelazzo MMZ, Pires BG, Marutani VHB, Xavier AAC, di Santis GW, Garcia JL, Alfieri AA (2018) Canine morbillivirus (canine distemper virus) with concomitant canine adenovirus, canine parvovirus-2, and *Neospora caninum* in puppies: a retrospective immunohistochemical study. Sci Rep 8(1):13477
29. Headley SA, Graça DL (2000) Canine distemper: epidemiological findings of 250 cases. Braz J Vet Res Anim Sci 37:136–140
30. Headley SA, Amude AM, Alfieri AF, Bracarense APRFL, Alfieri AA (2012) Epidemiological features and the neuropathological manifestations of canine distemper virus-induced infections in Brazil: a review. Semina Cienc Agrar 33(5):1945–1978
31. Headley SA, Alfieri AA, Fritzen JT et al (2013) Concomitant canine distemper, infectious canine hepatitis, canine parvoviral enteritis, canine infectious tracheobronchitis, and toxoplasmosis in a puppy. J Vet Diagn Investig 25(1):129–135
32. Guarner J, Brandt ME (2011) Histopathologic diagnosis of fungal infections in the 21st century. Clin Microbiol Rev 24(2):247–280
33. Sandoval-Denis M, Gene J, Sutton DA et al (2016) New species of *Cladosporium* associated with human and animal infections. Persoonia. 36:281–298
34. Sandoval-Denis M, Sutton DA, Martin-Vicente A, Cano-Lira JF, Wiederhold N, Guarro J, Gené J (2015) *Cladosporium* species recovered from clinical samples in the United States. J Clin Microbiol 53(9):2990–3000
35. Bensch K, Braun U, Groenewald JZ, Crous PW (2012) The genus *Cladosporium*. Stud Mycol 72:1–401
36. Bentley RT, Taylor AR, Thomovsky SA (2018) Fungal infections of the central nervous system in small animals: clinical features, diagnosis, and management. Vet Clin North Am Small Anim Pract 48(1):63–83
37. Bentley RT, Reese MJ, Heng HG, Lin TL, Shimonohara N, Fauber A (2013) Ependymal and periventricular magnetic resonance imaging changes in four dogs with central nervous system blastomycosis. Vet Radiol Ultrasound 54(5):489–496
38. Egelund GB, Ertner G, Kristensen LK et al (2017) Cerebrospinal fluid pleocytosis in infectious and noninfectious central nervous system disease: a retrospective cohort study. Medicine 96(18):e6686
39. Rakich PM, Latimer KS (2003) Cytology. In: Latimer KS, Mahaffey EA, Prasse KW (eds) Duncan and Prasse's Veterinary Laboratory Medicine: Clinical Pathology. Iowa State Press, Ames, pp 304–330
40. Garg N, Devi I, Vajramani G, Nagarathna S, Sampath S, Chandramouli BA, Chandramuki A, Shankar SK (2007) Central nervous system cladosporiosis: an account of ten culture-proven cases. Neurol India 55(3):282–288

41. Sharma RR, Pawar SJ, Lad SD, Mishra GP, Netalkar AS, Rege S (2012) Chapter 149 - fungal infections of the central nervous system. In: Quiñones-Hinojosa A (ed) Schmidek and sweet operative neurosurgical techniques, 6th edn. W.B. Saunders, Philadelphia, pp 1691–1732
42. Suri P, Chhina DK, Kaushal V, Kaushal RK, Singh J (2014) Cerebral phaeohyphomycosis due to *Cladophialophora bantiana* – a case report and review of literature from India. J Clin Diagn Res 8(4):DD01–DD05
43. Colombo AC, Rodrigues ML (2015) Fungal colonization of the brain: anatomopathological aspects of neurological cryptococcosis. An Acad Bras Cienc 87(2 Suppl):1293–1309
44. Gaunt MC, Taylor SM, Kerr ME (2009) Central nervous system blastomycosis in a dog. Can Vet J 50(9):959–962
45. Riet-Correa F, Krockenberger M, Dantas AF, Oliveira DM (2011) Bovine cryptococcal meningoencephalitis. J Vet Diagn Investig 23(5):1056–1060
46. Headley SA, Pimentel LA, Michelazzo MZ, Toma HS, Pretto-Giordano LG, Marcasso RA, Amude AM, Oliveira TE, Santos MD, Krockenberger M (2019) Pathological, histochemical and immunohistochemical findings associated with caprine pulmonary and encephalitic cryptococcosis. J Vet Diagn Investig 31(1):69–73
47. Curtis B, Hollinger C, Lim A, Kiupel M (2017) Embolic mycotic encephalitis in a cow following *Mortierella wolfii* infection of a surgery site. J Vet Diagn Investig 29(5):725–728
48. Schwerk C, Tenenbaum T, Kim KS, Schroten H (2015) The choroid plexus—a multi-role player during infectious diseases of the CNS. Front Cell Neurosci 9:80
49. Kovoor JM, Mahadevan A, Narayan JP et al (2002) Cryptococcal choroid plexitis as a mass lesion: MR imaging and histopathologic correlation. AJNR Am J Neuroradiol 23(2):273–276
50. Graciela Agar CH, Orozco Rosalba V, Macias Ivan C et al (2009) Cryptococcal choroid plexitis an uncommon fungal disease. Case report and review. Can J Neurol Sci 36(1):117–122
51. Habibi A, Safaiefarahani B (2018) Indoor damp surfaces harbor molds with clinical significance. Curr Med Mycol 4(3):1–9
52. Ascioglu S, Rex JH, de Pauw B, Bennett JE, Bille J, Crokaert F, Denning DW, Donnelly JP, Edwards JE, Erjavec Z, Fiere D, Lortholary O, Maertens J, Meis JF, Patterson TF, Ritter J, Selleslag D, Shah PM, Stevens DA, Walsh TJ, Invasive Fungal Infections Cooperative Group of the European Organization for Research and Treatment of Cancer, Mycoses Study Group of the National Institute of Allergy and Infectious Diseases (2002) Defining opportunistic invasive fungal infections in immunocompromised patients with cancer and hematopoietic stem cell transplants: an international consensus. Clin Infect Dis 34(1):7–14
53. Russell EB, Gunew MN, Dennis MM, Halliday CL (2016) Cerebral pyogranulomatous encephalitis caused by *Cladophialophora bantiana* in a 15-week-old domestic shorthair kitten. JFMS Open Rep 2(2):2055116916677935
54. (2017) Chapter 12 - Parvoviridae. In: MacLachlan NJ, Dubovi EJ (ed) Fenner's Veterinary Virology, 5th edn. Boston, Academic, pp 245–257
55. Revankar SG (2007) Dematiaceous fungi. Mycoses. 50(2):91–101